Experimental and numerical kinetic study of OME_2 and OME_3 combustion in low-pressure laminar flames

Yanan Huo*, Véronique Dias, Hervé Jeanmart

Institute of Mechanic, Materials and Civil Engineering (iMMC), Université catholique de Louvain, Belgium

Abstract

The urgency to reduce greenhouse gas emissions has motivated extensive research into renewable energy sources, particularly the studies on e-fuels, the liquid and gaseous fuels synthesized from electricity. Oxymethylene ethers (OMEs) have garnered significant attention as promising e-fuels within the context of the transition to sustainable energy systems, especially for the scenario of long-range transportation and extended storage. Understanding the oxidation kinetics of OMEs remains a prerequisite to optimizing their combustion. This study aims to elucidate the combustion chemistry and oxidation kinetics of longer-chain OMEs, namely OME_2 and OME_3. The premixed laminar stoichiometric flames of OME_2 and OME_3 are stabilized at 50 mbar and measured by molecular beam mass spectrometry (MBMS) in terms of speciation profiles. By following the reaction classes, a detailed mechanism including OME_2 is developed on the basis of our previous studies, which shows a good agreement with the experimental results of main species as well as important intermediates from OME_2 flames. It is observed that OME_1 chemistry plays a crucial role in the combustion of long-chain-length OMEs, and the species pool and reaction pathway of fuel oxidation is nearly independent of the chain length of OMEs.

Keywords: Oxymethylene ethers (OMEs); Molecular-beam mass spectrometry; Laminar Flames; Flat flames

1. Introduction

The urgency of reducing the emission of greenhouse gases and achieving a circular carbon economy encourages research on renewable energy systems. The liquid synthetic fuels, which are produced through water electrolysis and catalytic conversion with captured carbon dioxide (CO_2), a promising energy carrier contributing to the closed carbon cycle and especially to applications of long-distance transportation and long-term storage in the foreseeable future [1, 2]. Polyoxymethylene dimethyl ethers, also known as oxymethylene ethers (OMEs), with the general molecular structure $CH_3O(CH_2O)_nCH_3$, have been regarded as one of the most potentials candidates with the comparable physical and chemical properties to diesel fuel [3][4].

Compared to fossil diesel, the chain structure of OMEs contains C-O bonds with the lack of C-C bonds, contributing a high oxygen content (approximately 50%) and leading to significantly lower soot precursors formation such as C_2H_2, C_2H_4 and polycyclic-aromatic hydrocarbons (PAH) during combustion. OME_1, also called dimethoxymethane (DMM) or methylal, is usually applied as additives or blended with diesel fuel because of low cetane number, high volatility and low viscosity and lubricity [5]. However, as the chain length of OMEs increases, the properties of OMEs become competitive. When the number of CH_2O group is more than 2, the cetane number of OMEs is higher than that of diesel fuels following the potential replacement in terms of engine applications [6]. A thorough evaluation of the potential application of OMEs in engines or energy system necessitates an in-depth understanding of their fundamental combustion characteristics.

As the molecular with simplest linear structure in the OMEs group, OME_1 has been studied extensively by fundamental experiments in different combustion reactors, chemical kinetic modeling as well as theoretical calculations of relevant thermodynamic data and rate expressions [5, 7–15]. Fuel-lean (equivalence ratio of 0.24) and fuel-rich (equivalence ratio of 1.72) premixed OME_1/oxygen/argon flames under low pressure of 50 mbar were studied in our previous work which resulted in a new sub-mechanism of OME_1 added into the UCL mechanism including the formation and consumption of oxygenated species involved in OME_1 oxidation [7]. It was concluded that the pathway to primary fuel radical ($CH_3OCH_2O\dot{C}H_2$) formation is faster compared to the secondary radical ($CH_3O\dot{C}HOCH_3$) formation. Jacobs et al. developed a kinetic model of OME_1 oxidation at engine conditions by following the reaction classes method and was validated against experimental results of ignition delay time (IDT) in a shock tube and a rapid compression delay time (RCM), as well as a laminar flow reactor. It was concluded that the reactivity of OME_1 is controlled by the branching between two fuel radicals reaction pathways and is finally inhibited by the consumption of secondary fuel radicals over a wide range of temperatures. Alzueta et al. [12, 13] investigated OME_1 oxidation in a flow reactor at high and atmospheric pressures, from fuel-lean to rich conditions. The study at atmospheric pressure [12], with the interpretation of their chemical kinetic mechanism, shows that methyl formate (CH_3OCHO) is a vital intermediate and the activation energy value of the reaction of methyl formate conversion to methanol (CH_3OH) and carbon monoxide (CO) has a significant impact on the modeling results. The soot precursor, acetylene, was detected only under pyrolysis and very reducing conditions.

Few fundamental studies have been conducted on longer-chain species of OME_n ($n>1$) to characterize their combustion behaviour. The mechanism of OME_3 at low and intermediate temperatures for the prediction of the ignition characteristics was developed by He et al. [16] based on the reaction rates calculation with canonical transition state theory (CTST). Their mechanism has been validated against the results from experiments of a rapid compression machine and an HCCI with good agreement. Cai et al. [17] investigated the ignition delay time of $OME_{2\text{-}4}$ in a shock tube at pressures of 10 and 20 bar over the temperature range of 663-1137 K for equivalence ratios (Φ) of 0.5, 1.0, and 2.0. The chemical mechanism of $OME_{2\text{-}4}$ was obtained by using an automatic reaction class-based mechanism generator CLARA. C_0-C_4 mechanism from Blanquart et al. [18] was served as the base mechanism. To ensure the chemical validity, 21 reaction classes contemplated by Jacobs et al. [5] for OME_1 were specified for the generator to derive the elementary reactions of $OME_{2\text{-}4}$. The mechanism was optimized automatically concerning the calibrated rate rules for higher prediction accuracy. Concerning both models from He et al. [16] and Cai et al.[17] were not validated against experimental measurements of laminar flame speed, the updated mechanism including $OME_{1\text{-}3}$ pyrolysis and oxidation from Shretha et al. [3] was validated by the measurements of constant-volume chamber laminar flame speeds. The speciation study of OME_3 oxidation in a jet-stirred reactor was performed by Qiu et al. [19]. The experimental results were compared to the kinetics model from He et al. [16] and Cai et al. [17] with conclusions of the deviation on the mole fraction profiles of O_2 and intermediates at medium temperature. In the work from Wang et al. [14], pyrolysis of $OME_{1\text{-}3}$ was studied in a jet-stirred reactor at around atmospheric pressure (1.03 atm) and temperatures of 450-1080 K. The reactivity increases evidently with the increase of the fuel chain, reflected in the initial pyrolysis temperature decrease, which results from the production of CH_3 and H radicals from the unimolecular decomposition of $OME_{1\text{-}3}$. Methane and methyl formate were detected with high concentrations. They further investigated the low-temperature (500-950 K) oxidation kinetics of $OME_{1\text{-}3}$ [15]. It was found that, under low temperatures, OME_1 is directly decomposed into small molecules resulting in

a faster decomposition rate than that of OME_2 and OME_3. In the recent work, Ras et al. [20, 21] updated additional species and reactions along with new calculated thermodynamic and kinetic parameters for low-temperature oxidation of OME_2 and validated their new mechanism against experimental observations of stabilized ozone-seeded OME_2/dimethyl ether/oxygen premixed cool flames. However, the experimental speciation measurements of longer-chain OMEs in the stabilized burner are limited. Sun et al. [22] investigated the high-temperature combustion chemistry of stoichiometric OME_3 flat flame with a synchrotron vacuum ultraviolet photoionization mass spectrometry. The method of analogy was applied to construct the model for $OME_{1\text{-}3}$ showing good predictions of major species mole fraction profiles. Gaiser et al. [23] recently studied fuel-rich (Φ=1.7) premixed flames of $OME_{0\text{-}4}$ with electron ionization (EI) MBMS at 40 mbar with the help of kinetic modeling with the mechanism from Kathrotia et al. [24] for interpretation, making conclusion that oxygenated species dominate the combustion process and the observed species pool is nearly independent of the chain length of the respective OME_s. The agreement between experimental data from Gaiser et al. [23] and the model from Kathrotia et al. [24] prediction is sensible but not perfect, suggesting that the combustion chemistry of longer-chain OMEs at comprehensive conditions is not yet fully understood.

Both works from Sun et al. [22] and Gaiser et al. [23] are lack of the speciation measurements of longer-chain OMEs burner stabilized flames under fuel-lean conditions. The flat premixed low-pressure flame sampled by molecular-beam mass spectrometry (MBMS) with electron ionization (EI) is one of the most adaptable tools for chemical analysis of combustion systems. In this work, the combustion chemistry of OME_2 and OME_3 is investigated in detail experimentally and through kinetic modeling by using the extended mechanism. Speciation measurements are performed with MBMS in premixed laminar flames of OME_2 and OME_3 under stoichiometric at low pressure for the preparation of fuel-lean flames measurement of two fuels.

2. Experimental setup

Stoichiometric flames of OME_2 and OME_3 were stabilized at 50 bar with a total inlet flow rate of 5.72 slm on a stainless Spalding-Botha type burner in diameter of 80 mm. The burner was cooled to around 300 K and horizontally moveable with a range of 30 mm and precision of 0.1 mm. Table 1. shows the inlet composition of flames. Flows of oxygen and argon were adjusted by calibrated mass flow controllers (Bronkhorst, Mini Cori-Flow M12/$\pm$0.5% precision). Liquid fuel delivery was operated with a controlled evaporation and mixing system (CEM) from Bronkhorst. The fuels were stored in and drown from an ambient temperature tank which is pressurized at 2 bar with inert gas helium for its lower solubility than nitrogen to avoid from the formation of bubbles and to ensure constant flow, and were measured by a liquid flow meter (mini CORI-FLOW/$\pm$0.5% precision). The flow rate of carrier gas argon was 2 L/min. The temperature of the evaporation chamber was set to 383.15 K for OME_2 and 423.15 K for OME_3. OME_2 and OME_3 were purchased from ASG Analytik-Service with a purity of $>$98%. To avoid condensation, the gaseous mixture were then fed over a continuously heating pipe with a temperature of 473.14 K (8 mm inner diameter) before entering the combustion burner. The flames were sampled by a quartz cone with an opening angle of 45° and a 120 μm opening at the tip. The high vacuum chamber (10^{-5} mabr) behind the quartz cone forces the sampling gas to form a molecular beam, which is then sucked into the chamber of lower pressure (10^{-6} mbar), passes through a copper skimmer, and reaches the ionization chamber of the mass spectrometer (10^{-7} mbar). The axis of the mass spectrometer is perpendicular to the molecular beam. This arrangement allows the gaseous sample to be "frozen" to keep chemical composition unchanged from the tip of the cone to the detection system and enables the detection of reactive chemical species avoiding reactions with other molecules or the wall. In order to minimize interferences from fragmentation during ionization with electrons or from overlapping species with similar masses, the ionization potentials were measured and chosen specifically for the species detected with the precision of 0.01 eV. For OME_n (n$>$0), it is difficult to form stable molecular ions in the MBMS. The signal of molecular $C_4H_9O_3$ was regarded as OME_2 and OME_3.

Conversion of signal intensities to mole fraction profiles was performed using a calibrated mixture for stable compounds and estimating ionization cross-sections for radicals and unstable species. An internal calibration procedure was used for the calibration of the major species, such as fuel, O_2, CO_2, CO, H_2 and H_2O. The direct calibration was used for the determination of CH_4. The method of relative ionization cross sections (RICS) wes used for the determination of other intermediates. The uncertainty associated with the procedure is estimated to be less than 30%. Estimating ionization cross-sections for unstable species resulted in uncertainties by a factor of 2.

The temperature profiles of both OME_2 and OME_3 premixed laminar flames were measured with a customized fine B-type thermocouple composed of PtRh6%-PtRh30% with a diameter of 0.42 mm for wires and a diameter of 1.31 mm for the bead. The thermocouple bead was placed in front of the sampling quartz nozzle and parallel to the burner surface. The obtained raw temperature profiles were corrected for radiation losses to get accurate temperatures.

3. Chemical kinetic modeling

In this work, two mechanisms were used for chemical kinetic modelling. The mechanism proposed

Table 1: Compositions of inlet flow (slm at 273 K; 1.01 bar), and italics in the brackets are mole fractions

Fuel	Φ	Fuel(g/h)	O_2(slm)	Ar(slm)
OME_2	1.00	55 (*0.04*)	1.06 (*0.20*)	4.44 (*0.76*)
OME_3	1.00	73 (*0.04*)	1.33 (*0.23*)	4.17 (*0.73*)

here, which includes the OME_2 and work-in-progress sub-mechanism of OME_3, extends our previous work from Dias et al. [7], which was developed to predict OME_1 combustion. The UCL mechanism[7] was validated against the measurements of lean and rich premixed laminar flames of $OME_1/O_2/Ar$ under low-pressure of 50 mbar. It has been demonstrated that the kinetic model satisfactorily predicted the oxidation of OME_1 and analyzed its consumption pathway. The active reaction sites are the carbon atoms in both structures of OMEs and alkanes where oxygen addition and inter- or intramolecular hydrogen transfer happen, especially under low temperatures. With the existence of C-O, carbonyl species are produced once a double bond is formed instead of alkenes formation from alkanes. Based on this assumption of an analogy to regular alkanes, the establishment of sub-mechanisms of OME_2 and OME_3 in this study followed the reaction classes method referred to Jacobs et al. [5]. The sub-mechanism of OME_1 has been expanded with low-temperature reaction classes, such as fuel radicals decomposition to carbonyl molecule, first addition of oxygen to form RO_2, isomerization of RO_2 to QOOH and so on. The sub-mechanism of dimethyl carbonate ($CH_3OCOOCH_3$), formic anhydride (OCHOCHO), and methyl formate (CH_3OCHO) has been expanded. Only high-temperature reaction classes were considered and introduced into the OME_2 sub-mechanism. In this study, The main OME_2 and OME_3 sub-mechanisms are based on the modeling work of Cai et al. [17] and Sun et al. [22], including the reaction classes of unimolecular decomposition of fuel, hydrogen abstraction and β-scission of fuel molecules and radicals. The formation and consumption pathways of important intermediates methoxymethyl formate (CH_3OCH_2CHO) were added. However, the implementation of their sub-mechanisms in the UCL mechanism without any changes could not provide a satisfactory performance against experiment results for one of the reasons of different base chemistry.

At the same time, the mechanism from Kathrotia et al. [24], which includes ethers from OME_0 to OME_5 with 1814 reactions and 238 species, was used for comparison with the speciation measurements of OME_2 and OME_3 flames [23]. It is named Kath-mechanism in the following discussion. The numerical modeling is performed using OpenSMOKE++[25].

4. Result and discussion

In the following figures, the symbols are experimental data from this work and the lines are simulation results. Two models were applied for the simulation of stoichiometric OME_2 flame, which are the new UCL mechanism for this work and Kathrotia et al. [24] named as Kath-mechanism. The Kath-mechanism was the only mechanism used to predict OME_3 stoichiometric flame.

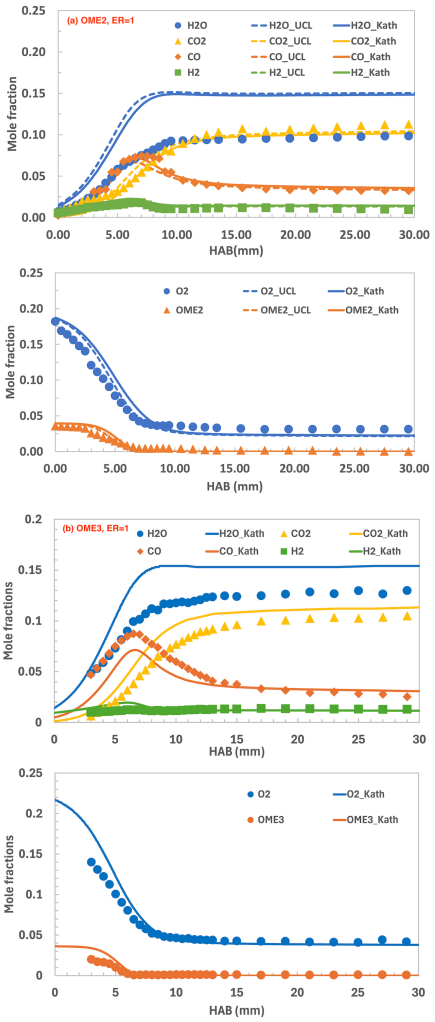

Fig. 1: Main species experimental mole fraction profiles (dots) of OME_2 and OME_3 flames compared to simulation results (lines)

Fig. 1 shows the experimental and numerical results of the main products of the stoichiometric flames of OME_2 and OME_3. The trend and magnitude of the main species and reactants were predicted excellently by both kinetic models. It can be observed by the peak positions of CO and H_2 to guess that OME_3 is consumed slightly faster compared to OME_2. The proximity of the reaction zone makes the increasing gas phase near the burner surface, leading to fuel decomposition at a lower temperature and closer to the burner surface.

Fig. 2 and Fig. 3 show the mole fraction profiles of HCO and HO_2 of two flames. In the OME_2 flame, Kath-mechanism showed a good agreement with the mole fraction of HO_2, however, UCL-mechanism underestimated the concentration of HO_2. In terms of HCO mole fraction profile, both mechanisms underestimated the mole fraction but with a good prediction of peak position. In the OME_3 flame, Kath-mechanism slightly overestimated the mole fraction of HO_2. The magnitude of the HCO mole fraction was well estimated by Kath-mechanism with an unfortunate shifted peak position.

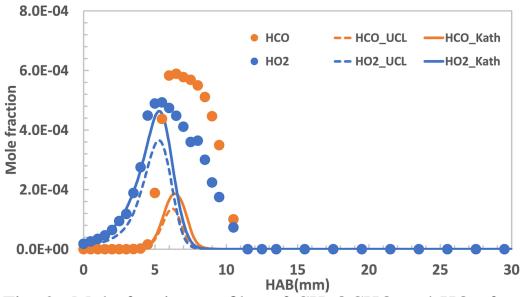

Fig. 2: Mole fraction profiles of CH_3OCHO and HO_2 for OME_2 stoichiometric flame compared to numerical results from UCL-mechanism and Kath-mechanism.

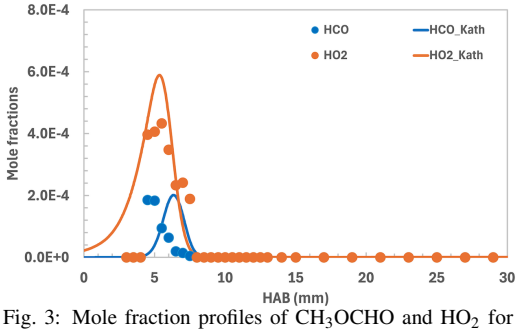

Fig. 3: Mole fraction profiles of CH_3OCHO and HO_2 for OME_3 stoichiometric flame compared to numerical results from Kath-mechanism.

In the combustion of OMEs, oxygenated species are the dominated intermediates. Small oxygenated species which are important in the OME_1 combustion also play a crucial role in the combustion processes of OME_2 and OME_3. All OMEs consumption primarily starts with the abstraction of a terminal H or the unimolecular decomposition, for the reason that the bond dissociation energy of the C-O in the terminal moieties -OCH_3 is lower than in the middle moieties -CH_2O- [22]. Therefore, the intermediates CH_3OCHO and CH_3OCH_2CHO are important during OMEs combustion. Unfortunately, it was difficult to obtain stable mole fraction profiles lower than 0.1 ppm with current analyzing equipment. The intermediate CH_3OCH_2OCHO mole fraction profile was absent in this study. The possible reason could be the fast consumption or unimolecular decomposition of CH_3OCH_2CHO. In Fig. 4, the results from Kath-mechanism show good agreement with the experimental results of CH_3OCHO in OME_2 and OME_3 flames. However, UCL-mechanism highly overestimated the mole fraction of CH_3OCHO in OME_2 flame. One of the possible reasons for large discrepancies between model-predicted results and experimental measurements could be the multivariate formation pathway of CH_3OCHO in our study compared to Kath-mechanism. In the Kath-mechanism, CH_3OCHO only formed from the decomposition of secondary radicals of $OME_{1\text{-}3}$ below:

$$OME_1 * 2 = CH_3OCHO + CH_3 \quad (1)$$

$$OME_2 * 2 = CH_3OCHO + CH_3OCH_2 \quad (2)$$

$$OME_3 * 2 = CH_3OCHO + OME_1 * 1 \quad (3)$$

It requires future studies on completing the consumption and formation pathway of CH_3OCHO and, if necessary, studies on associated thermodynamic parameters and reaction rate coefficients.

With the lack of C-C bonds in the fuel molecules, the main formation pathways for species with C-C bonds are generally initiated by recombination of CH_3 radicals which are immediately formed during the oxidation. In Fig. 4, it also shows the mole fraction profile of C_2H_6 in OME_2 flame. Both kinetic models overestimated the mole fraction of C_2H_6 and predicted the narrower width compared to the experimental data.

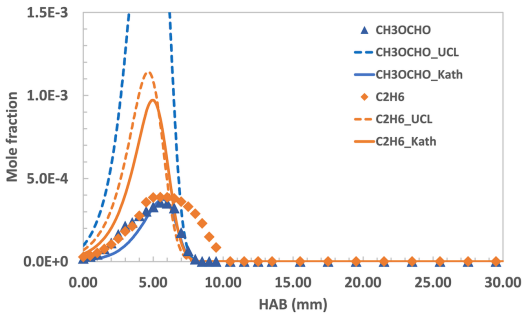

Fig. 4: Mole fraction profiles of CH_3OCHO and C_2H_6 for OME_2 stoichiometric flame compared to numerical results from UCL-mechanism and Kath-mechanism.

In Fig. 5, the Kath-mechanism showed good performance on predicting both the mole fraction and peak position of CH_3OCHO in OME_3. It was surprisingly found that the species $CH_3OCH_2O_2$ was detected in the stoichiometric OME_3 flame. However, the Kath-mechanism underestimated its mole fraction. The main formation of $CH_3OCH_2O_2$ is the reaction:

$$CH_3OCH_2 + O_2 <=> CH_3OCH_2O_2 \quad (4)$$

It is then consumed through unimolecular decomposition or the reaction with CH_2O or CH_3CHO. The

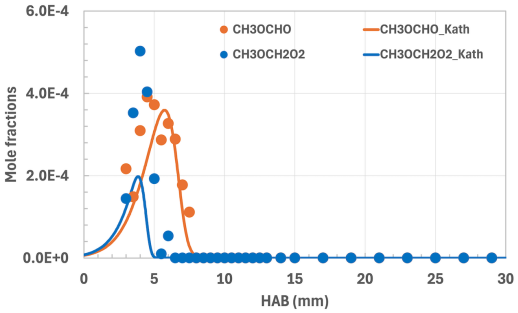

Fig. 5: Mole fraction profiles of CH_3OCHO and $CH3_2OCH_2O_2$ for OME_3 stoichiometric flame compared to numerical results from Kath-mechanism.

formation of CH_3OCH_2 species is mainly through the decomposition of fuel and fuel radicals. This discrepancy shows the lack of theoretical or experimental study on associated sub-mechanisms.

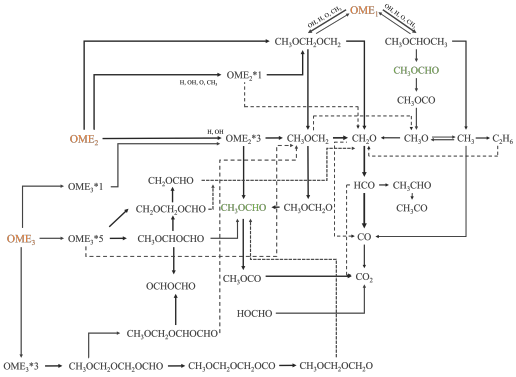

Fig. 6: Reaction pathway of OME_2 and OME_3 consumption and formation of intermediates in stoichiometric laminar flames with Kath-mechanism.

The Kath-mechanism was used to analyzed the reaction pathway of OME_2 and OME_3 consumption and formation of essential intermediates, as shown in Fig. 6. OME_1 decomposes to primary and secondary radicals followed by further decomposition to produce the fuel radical of OME_0. OME_2 undergoes either the unimolecular decomposition or H abstraction leading to its fuel radicals or primary radical of OME_1. It happens similarly on OME_3. The decomposition of OME_3 leads to fuel radicals of itself, OME_2 and OME_1 at an early stage. With the same conclusion as Shrestha et al. [3], the O_2 addition channel was mainly favoured under low temperatures. In this study, it is observed that OME_1 chemistry plays a crucial role in the combustion of long-chain-length OMEs. As same as the conclusion from Gaiser et al. [23] and Shrestha et al. [3], the species pool and reaction pathway of fuel oxidation is nearly independent of the chain length of OMEs. The primary decomposition channels of OME_2 and OME_3 in this study are the same as the observation of OME_1 oxidation studies.

5. Work in progress

The measurement of fuel-lean flames of OME_2 and OME_3 has been finished. The sub-mechanisms of OME_2 and OME_3 suitable to low-pressure premixed laminar flames have been established but require further modification, optimization and refinement with the help of our experimental data. The inclusive UCL-mechanism will be finished with the expended conditions of temperature and pressure and will be validated against the comprehensive experimental data.

6. Conclusion

In this work, the stoichiometric premixed laminar flames of OME_2 and OME_3 were detected and analyzed by molecular-beam mass spectrometry at 50 mbar. The mole fraction profiles of species, especially the reactive intermediates, were measured and presented. Numerical modeling was performed through applying UCL-mechanism with new-added OME_2 sub-mechanism and Kath-mechanism. The comparison between the experimental results of the two flames and simulations showed good agreement. With the reaction pathway analysis, it is observed that OME_1 chemistry plays a crucial role in the combustion of long-chain-length OMEs, and the species pool and reaction pathway of fuel oxidation is nearly independent of the chain length of OMEs. The sub-mechanisms of OME_2 and OME_3 still require further modification and optimization to get better predictions under the extended range of conditions.

Declaration of competing interest

The authors declare that they have no known competing financial interests or personal relationships that could have appeared to influence the work reported in this paper.

Acknowledgments

The authors are very grateful for the financial support from Fonds de la Recherche Scientifique-FNRS under grant n°T.0119.21.

References

[1] D. Bongartz, J. Burre, A. Mitsos, Production of oxymethylene dimethyl ethers from hydrogen and carbon dioxide—part i: Modeling and analysis for ome1, Industrial & Engineering Chemistry Research 58 (12) (2019) 4881–4889.

[2] Y. Fenard, G. Vanhove, A mini-review on the advances in the kinetic understanding of the combustion of linear and cyclic oxymethylene ethers, Energy & Fuels 35 (18) (2021) 14325–14342.

[3] K. P. Shrestha, S. Eckart, S. Drost, C. Fritsche, R. Schießl, L. Seidel, U. Maas, H. Krause, F. Mauss, A comprehensive kinetic modeling of oxymethylene

ethers (omen, n=1–3) oxidation - laminar flame speed and ignition delay time measurements, Combustion and Flame 246 (2022) 112426.

[4] H. Liu, Z. Wang, J. Zhang, J. Wang, S. Shuai, Study on combustion and emission characteristics of polyoxymethylene dimethyl ethers/diesel blends in light-duty and heavy-duty diesel engines, Applied Energy 185 (2017) 1393–1402, clean, Efficient and Affordable Energy for a Sustainable Future.

[5] S. Jacobs, M. Döntgen, A. B. Alquaity, W. A. Kopp, L. C. Kröger, U. Burke, H. Pitsch, K. Leonhard, H. J. Curran, K. A. Heufer, Detailed kinetic modeling of dimethoxymethane. part ii: Experimental and theoretical study of the kinetics and reaction mechanism, Combustion and Flame 205 (2019) 522–533.

[6] Z. Ren, C. Zhou, Z. Qiu, Y. Duan, D. Han, Unveiling high-temperature oxidation kinetics of pode2: Theoretical studies on the h-abstraction, isomerization, and -dissociation reactions, Combustion and Flame 262 (2024) 113360.

[7] V. Dias, X. Lories, J. Vandooren, Lean and rich premixed dimethoxymethane/oxygen/argon flames: Experimental and modeling, Combustion Science and Technology 182 (4-6) (2010) 350–364.

[8] W. Sun, T. Tao, M. Lailliau, N. Hansen, B. Yang, P. Dagaut, Exploration of the oxidation chemistry of dimethoxymethane: Jet-stirred reactor experiments and kinetic modeling, Combustion and Flame 193 (2018) 491–501.

[9] W. A. Kopp, L. C. Kröger, M. Döntgen, S. Jacobs, U. Burke, H. J. Curran, K. Alexander Heufer, K. Leonhard, Detailed kinetic modeling of dimethoxymethane. part i: Ab initio thermochemistry and kinetics predictions for key reactions, Combustion and Flame 189 (2018) 433–442.

[10] F. H. Vermeire, H.-H. Carstensen, O. Herbinet, F. Battin-Leclerc, G. B. Marin, K. M. V. Geem, Experimental and modeling study of the pyrolysis and combustion of dimethoxymethane, Combustion and Flame 190 (2018) 270–283.

[11] C. A. Daly, J. M. Simmie, P. Dagaut, M. Cathonnet, Oxidation of dimethoxymethane in a jet-stirred reactor, Combustion and Flame 125 (3) (2001) 1106–1117.

[12] L. Marrodán, F. Monge, Ángela Millera, R. Bilbao, M. U. Alzueta, Dimethoxymethane oxidation in a flow reactor, Combustion Science and Technology 188 (4-5) (2016) 719–729.

[13] L. Marrodán, E. Royo, Millera, R. Bilbao, M. U. Alzueta, High pressure oxidation of dimethoxymethane, Energy & Fuels 29 (5) (2015) 3507–3517.

[14] X. Zhong, H. Wang, Q. Zuo, Z. Zheng, J. Wang, W. Yin, M. Yao, Experimental and kinetic modeling studies of polyoxymethylene dimethyl ether (pode) pyrolysis in jet stirred reactor, Journal of Analytical and Applied Pyrolysis 159 (2021) 105332.

[15] H. Wang, Z. Yao, X. Zhong, Q. Zuo, Z. Zheng, Y. Chen, M. Yao, Experimental and kinetic modeling studies on low-temperature oxidation of polyoxymethylene dimethyl ether (dmm1-3) in a jet-stirred reactor, Combustion and Flame 245 (2022) 112332.

[16] T. He, Z. Wang, X. You, H. Liu, Y. Wang, X. Li, X. He, A chemical kinetic mechanism for the low- and intermediate-temperature combustion of polyoxymethylene dimethyl ether 3 (PODE3), Fuel 212 (2018) 223–235.

[17] L. Cai, S. Jacobs, R. Langer, F. vom Lehn, K. A. Heufer, H. Pitsch, Auto-ignition of oxymethylene ethers (OMEn, n = 2–4) as promising synthetic e-fuels from renewable electricity: shock tube experiments and automatic mechanism generation, Fuel 264 (2020) 116711.

[18] G. Blanquart, P. Pepiot-Desjardins, H. Pitsch, Chemical mechanism for high temperature combustion of engine relevant fuels with emphasis on soot precursors, Combustion and Flame 156 (3) (2009) 588–607.

[19] Z. Qiu, A. Zhong, Z. Huang, D. Han, An experimental and modeling study on polyoxymethylene dimethyl ether 3 (pode3) oxidation in a jet stirred reactor, Fundamental Research 2 (5) (2022) 738–747.

[20] K. De Ras, M. Kusenberg, G. Vanhove, Y. Fenard, A. Eschenbacher, R. J. Varghese, J. Aerssens, R. Van de Vijver, L.-S. Tran, J. W. Thybaut, K. M. Van Geem, A detailed experimental and kinetic modeling study on pyrolysis and oxidation of oxymethylene ether-2 (ome-2), Combustion and Flame 238 (2022) 111914.

[21] K. De Ras, T. Panaget, Y. Fenard, J. Aerssens, L. Pillier, J. W. Thybaut, G. Vanhove, K. M. Van Geem, An experimental and kinetic modeling study on the low-temperature oxidation of oxymethylene ether-2 (ome-2) by means of stabilized cool flames, Combustion and Flame 253 (2023) 112792.

[22] W. Sun, G. Wang, S. Li, R. Zhang, B. Yang, J. Yang, Y. Li, C. K. Westbrook, C. K. Law, Speciation and the laminar burning velocities of poly(oxymethylene) dimethyl ether 3 (POMDME3) flames: An experimental and modeling study, Proceedings of the Combustion Institute 36 (1) (2017) 1269–1278.

[23] N. Gaiser, H. Zhang, T. Bierkandt, S. Schmitt, J. Zinsmeister, T. Kathrotia, P. Hemberger, S. Shaqiri, T. Kasper, M. Aigner, P. Oßwald, M. Köhler, Investigation of the combustion chemistry in laminar, low-pressure oxymethylene ether flames (ome0–4), Combustion and Flame (2022) 112060.

[24] T. Kathrotia, P. Oßwald, J. Zinsmeister, T. Methling, M. Köhler, Combustion kinetics of alternative jet fuels, part-III: Fuel modeling and surrogate strategy, Fuel 302 (2021) 120737.

[25] A. Cuoci, A. Frassoldati, T. Faravelli, E. Ranzi, Opensmoke++: An object-oriented framework for the numerical modeling of reactive systems with detailed kinetic mechanisms, Computer Physics Communications 192 (2015) 237–264.